First Measurement of the ^{64}Ni$(\gamma, n)^{63}$Ni Cross Section

I. Dillmann$^{* \dagger \ddagger}$ **T. Faestermann, G. Korschinek, J. Lachner** § **M. Maiti** ¶ **M. Poutivtsev, G. Rugel**

Physik-Department and Excellence Cluster Universe, D-85748 Garching, Germany

S. Walter, F. Käppeler

Karlsruhe Institute of Technology, Campus Nord, Institut für Kernphysik, D-76021 Karlsruhe, Germany

M. Erhard $^{\|}$ **A.R. Junghans, C. Nair** ** **R. Schwengner, A. Wagner**

Institut für Strahlenphysik, Helmholtz-Zentrum Dresden-Rossendorf e.V., Bautzner Landstrasse 400, D-01328 Dresden, Germany

M. Pignatari

Joint Institute for Nuclear Astrophysics, University of Notre Dame, Notre Dame, IN 46556, USA
Department of Physics & Astronomy, University of Victoria, Victoria, BC V8P5C2 Canada
TRIUMF, 4004 Wesbrook Mall, Vancouver, BC V6T2A3, Canada

T. Rauscher

Department of Physics, University of Basel, Klingelbergstrasse 82, CH-4056 Basel, Switzerland

A. Mengoni

ENEA Bologna, Italy

In the past 10 years new and more accurate stellar neutron capture cross section measurements have changed and improved the abundance predictions of the weak s process. Among other elements in the region between iron and strontium, most of the copper abundance observed today in the solar system distribution was produced by the s process in massive stars. However, experimental data for the stellar $^{63}\text{Ni}(n,\gamma)^{64}\text{Ni}$ cross section are still missing, but is strongly required for a reliable prediction of the copper abundances.

^{63}Ni ($t_{1/2}$=101.2 a) is a branching point and also a bottleneck in the weak s process flow, and behaves differently during core He and shell C burning. During core He burning the reaction flow proceeds via β-decay to ^{63}Cu, and a change of the $^{63}\text{Ni}(n,\gamma)^{64}\text{Ni}$ cross section would have no influence. However, this behavior changes at higher temperatures and neutron densities during the shell C burning phase. Under these conditions, a significant amount of the s process nucleosynthesis flow is passing through the channel $^{62}\text{Ni}(n,\gamma)^{63}\text{Ni}(n,\gamma)^{64}\text{Ni}$.

At present only theoretical estimates are available for the $^{63}\text{Ni}(n,\gamma)^{64}\text{Ni}$ cross section. The corresponding uncertainty affects the production of ^{63}Cu in present s process nucleosynthesis calculations and propagates to the abundances of the heavier species up to A=70. So far, experimental information is also missing for the inverse $^{64}\text{Ni}(\gamma,n)$ channel. We have measured for the first time the $^{64}\text{Ni}(\gamma,n)^{63}\text{Ni}$ cross section and also combined for the first time successfully the photoactivation technique with subsequent Accelerator Mass Spectrometry (AMS). The activations at the ELBE facility in Dresden-Rossendorf were followed by the $^{63}\text{Ni}/^{64}\text{Ni}$ determination with AMS at the MLL accelerator laboratory in Garching. First results indicate that theoretical predictions have overestimated this cross section up to now. If this also holds for the inverse channel $^{63}\text{Ni}(n,\gamma)^{64}\text{Ni}$, more ^{63}Ni is accumulated during the high neutron density regime of the C shell that will contribute to the final abundance of ^{63}Cu by radiogenic decay. In this case, also a lower s process efficiency is expected for the heavier species along the neutron capture path up to the Ga-Ge region.

*Speaker.

†Now at II. Physikalisches Institut, Justus-Liebig Universität Giessen and GSI Helmholtzzentrum für Schwerionenforschung, Darmstadt, Germany; Previous affiliation: Karlsruhe Institute of Technology, Campus Nord, Institut für Kernphysik, D-76021 Karlsruhe, Germany

‡This research is supported by the DFG cluster of excellence "Origin and Structure of the Universe". I.D. is supported by the Helmholtz society via the Young Investigators project VH-NG-627.

§Now at Labor für Ionenstrahlphysik, ETH Zürich, Switzerland

¶Now at Saha Institute of Nuclear Physics, Chemical Sciences Division, 1/AF Bidhannagar, Kolkata, India

‖Now at Physikalisch-Technische Bundesanstalt (PTB), Bundesallee 100, D-38116 Braunschweig, Germany

**Now at Argonne National Laboratory, USA

1. Introduction

The nucleosynthesis of elements heavier than iron can be almost completely ascribed to the *s* process ("slow neutron capture process") and the *r* process ("rapid neutron capture process") [1]. The *s* process can be further divided into a "weak" component (responsible for nuclei up to $A \approx 90$) and a "main" component (for $90 < A < 209$), which occur in different astrophysical scenarios at different temperatures and with different neutron exposures. The weak *s* process occurs during core He and shell C burning in massive stars. Among the nuclei involved, the long-lived isotopes ^{63}Ni, ^{79}Se, and ^{85}Kr take key positions, because their stellar β^--decay rate becomes comparable to the neutron capture rate ($\lambda_\beta \approx \lambda_n$). The resulting competition leads to branchings in the *s* process nucleosynthesis path.

The branching ratio

$$f_b = \frac{\lambda_\beta}{\lambda_\beta + \lambda_n} \tag{1.1}$$

determines whether neutron capture ($f_b < 0.5$) or β-decay ($f_b > 0.5$) is preferred. During core He burning, moderate conditions with temperatures of $T \approx 300$ MK and neutron densities in the order of 10^6 cm^{-3} are reached. The reaction flow of the weak *s* process cannot bridge the radioactive ^{63}Ni and thus has to wait for the β-decay into ^{63}Cu. The branching ratio is $f_b = 0.91$ [2] and the reaction flow "branches" later at ^{64}Cu ($t_{1/2} = 12.7$ h) which is an isotopes which can decay by electron capture (61.5%) and also by β^--decay (38.5%).

However, this situation changes drastically during shell C burning [3]. At temperatures up to $T = 1$ GK and neutron densities beyond 10^{11} cm^{-3} neutron captures on ^{63}Ni become possible and the reaction path is driven 2-3 units away from stability ($f_b = 0.02$ [2]). The different reaction paths during these burning phases are shown in Fig. 1. As can be seen only during the shell C burning phase, a change in the ^{63}Ni$(n,\gamma)^{64}$Ni cross section affects the weak *s* process flow towards higher masses, and ^{63}Cu is only produced via radiogenic decay of ^{63}Ni.
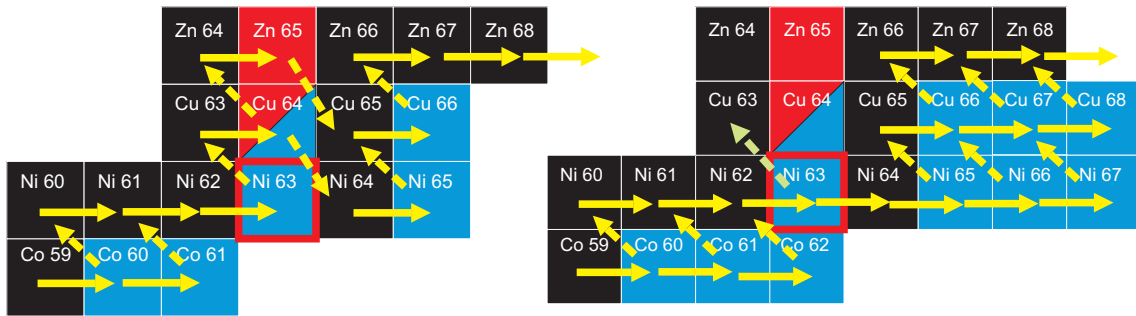

Figure 1: Weak *s* process around ^{63}Ni during the core He (left) and shell C burning phase (right).

The propagation effects induced by changes of single cross sections in the weak *s* process were first observed in the case of ^{62}Ni$(n,\gamma)^{63}$Ni [4]. The previously recommended stellar cross section for $kT = 30$ keV [5] was almost a factor of 2 lower than results of recent measurements [6] using either the activation technique and subsequent Accelerator Mass Spectrometry (AMS) [2, 7, 4] or the time-of-flight technique [8]. This change of a single cross section led not only to a 20% reduction of the ^{62}Ni abundance, but propagated up to $A = 90$ causing a 20% increase

2

of the abundances of the heavier isotopes [4]. The reason for this strong influence of changes in single cross sections is that the weak *s* process is – unlike the main *s* process component – not in equilibrium and thus the relation $N \times \sigma = const.$ does not hold. Low cross sections (below 150 mb) act as bottlenecks and induce a propagation effect towards higher masses up to the N=50 shell closure.

Recent stellar simulations [3] using new experimental neutron capture data published since the release of the Bao et al. compilation [5] identified other bottlenecks, e.g. ^{60}Ni, ^{63,65}Cu, ^{74}Ge, and ^{78}Se. Fig. 10 in Ref. [3] shows the result of these "combined" propagation effects on the nucleosynthesis yields after core He and shell C burning.

An accurate knowledge of the $^{63}\text{Ni}(n,\gamma)^{64}\text{Ni}$ cross section is also strongly required for the prediction of the abundances of the copper isotopes ^{63,65}Cu. Pignatari et al. [3] showed in their Fig. 14 that the largest uncertainty comes from the yet unmeasured $^{63}\text{Ni}(n,\gamma)^{64}\text{Ni}$ cross section. They also showed (for a 25 M$_\odot$ star after shell C burning) that the solar ratios of ^{63}Cu and ^{65}Cu (69.17% and 30.83%, respectively) are best reproduced if the theoretical prediction from the Hauser-Feshbach code NON-SMOKER [9] is reduced by a factor of two. Since no experimental data is available for this cross section up to now, we tried to set first experimental constraints by measuring the inverse reaction channel, $^{64}\text{Ni}(\gamma,n)$.

2. Experimental procedure and preliminary results

The photoactivation of enriched ^{64}Ni samples was performed at the ELBE accelerator at Helmholtz-Zentrum Dresden-Rossendorf using bremsstrahlung spectra with three different end point energies. The ELBE source delivers continuous wave electron beams with a maximum total energy of 40 MeV at a maximum average current of 1 mA [10].

Electrons are pre-accelerated in a 250 keV-thermionic DC electron-gun and pre-bunched in two Radio-Frequency (RF) buncher sections. Main acceleration is accomplished in two 20 MeV-superconducting linear accelerator modules operated at 1.3 GHz. Two 9-cell superconducting niobium cavities are operated in a cryo-module with superfluid liquid helium at a temperature of 1.8 K. Each cavity is driven by a 10 kW klystron amplifier. The maximum accelerating gradient is 15 MV/m.

The bremsstrahlung facility is located before the second linac module and can use a maximum energy of 20 MeV. The primary electron beam is deflected from the main beamline onto a thin Nb foil and produces bremsstrahlung via deceleration of electrons [11]. The radiator converts the kinetic energy of only a small fraction of the electrons to bremsstrahlung while the main fraction passes the radiator and is separated from the photon beam by a dipole magnet. After deflection, the electron beam is led through a thin vacuum separation window made from beryllium and dumped into the graphite electron beam dump (photoactivation site). The photon flux can reach here up to 10^{10}cm^{-2}s^{-1}MeV^{-1}, thus the ^{64}Ni samples were irradiated at this position together with the activation standard target ^{197}Au.

The bremsstrahlung produced in the Nb radiator continues straight through the collimator to the photon scattering site, where a ^{11}B sample is irradiated together with the activation standard target ^{197}Au. The scattered photons from known resonances in ^{11}B are observed by means of HPGe detectors for the experimental determination of the absolute photon flux. The activation of ^{197}Au

is a measure of the integrated photon flux up to the endpoint energy and is also used to relate the photon flux intensity to the one at the activation site inside the electron beam dump.

The endpoint energy of the bremsstrahlung distribution is determined by measuring the proton energy spectrum from the deuteron breakup with silicon detectors. We have performed three photoactivations at endpoint energies of E_0=13.4, 11.5, and 10.3 MeV. The time-integrated photon flux was in all three cases in the order of 10^{14} cm^{-2} MeV^{-1}. The resulting reaction yield $Y_{act} = \frac{^{63}Ni}{^{64}Ni}$ was then measured with Accelerator Mass Spectrometry (AMS).

The AMS measurements were performed with the gas-filled analyzing magnet system (GAMS) at the 14 MV MP tandem accelerator of the Maier-Leibnitz-Laboratory in Garching/ Germany. The setup for ^{63}Ni consists of a cesium sputter ion source dedicated exclusively to this isotope with an isobaric ^{63}Cu background smaller by 2 orders of magnitude compared to the standard ion sources [12, 13]. The sample materials were an amorphous Ni powder (99.63% ^{64}Ni), used for the activations at E_0=13.4 and 11.5 MeV, and a metal foil (89.6% ^{64}Ni), used for the activation at E_0=10.3 MeV. The samples were pressed into ultrapure graphite cathodes without further chemical processing. The nickel was extracted from the ion source as Ni$^-$ and stripped to positive charge states by a thin carbon foil (4 μg/cm^2) at the terminal of the tandem accelerator. For the measurements the 12$^+$ and 13$^+$ charge states and terminal voltages between 12.2 and 12.7 MV were chosen. The GAMS detection system consists of a 135° gas-filled magnet and a Frisch-grid ionization chamber, where the anode is divided along the flight path into five energy loss signals $\Delta E1$ to $\Delta E5$. The field of the GAMS magnet was adjusted to suppress the remaining ^{63}Cu background as much as possible without hampering the ^{63}Ni measurement. This combination allows the determination of ^{63}Ni/Ni ratios as low as 2×10^{-14}, with a total isobaric suppression of several 10^9 [12, 13].

The activated samples, blank samples, and standards were measured alternately several times under the same conditions. The sample activated with bremsstrahlung at E_0=13.4 MeV yielded $Y_{act} = \frac{^{63}Ni}{^{64}Ni} = (1.5\pm0.4)\times10^{-12}$, well above the background of 8×10^{-14}. This result is in good agreement with the previous measurement of $\frac{^{63}Ni}{^{64}Ni} = (1.1^{+0.5}_{-0.4})\times10^{-12}$ reported in Refs. [2, 7]. The second sample activated at an endpoint energy of E_0=11.5 MeV was measured for the first time and had a factor of 2 higher background. The resulting isotope ratio was $\frac{^{63}Ni}{^{64}Ni} = (3.7\pm2.1)\times10^{-13}$ after background subtraction. The third sample at E_0=10.3 MeV suffered from an even higher intrinsic background and could not yet be analyzed.

These experimental reaction yields can now be compared with "theoretical" reaction yields (normalized to the respective photon fluence) using the cross sections from the codes NON-SMOKER [14] and Talys [15]. This is done via the factor $k_{norm} = \frac{Y_{act}(exp)}{Y_{act}(theo)}$. As can be seen in Table 1, our experimental results are lower by factors of 1.5–4 than the predictions, and seem also to have a different energy dependence (the factor k_{norm} is not constant). However, a final conclusion has to await the repetition of the AMS measurements and inclusion of the third sample in the near future.

3. Summary

We have measured for the first time the ^{64}Ni(γ,n) cross section by combining the photoactivation technique with Accelerator Mass Spectrometry. Our results imply that this cross section is smaller than previously predicted by the NON-SMOKER [14] and TALYS [15] codes (Table 1).

Table 1: Preliminary results of the ${}^{64}Ni(\gamma,n){}^{63}Ni$ measurements for the two samples activated at endpoint energies of 13.4 and 11.5 MeV and comparison with theoretical predictions from Talys 1.2 [15] and NON-SMOKER [14].

E_0	Exp.	Talys 1.2		NON-SMOKER	
(MeV)	Y_{act}(exp)	Y_{act}(T)	k_{norm}(T)	Y_{act}(NS)	k_{norm}(NS)
11.5	$(3.7\pm2.1)\times10^{-13}$	$(1.6\pm0.1)\times10^{-12}$	0.23 ± 0.13	$(8.2\pm0.3)\times10^{-13}$	0.45 ± 0.26
13.4	$(1.5\pm0.4)\times10^{-12}$	$(3.6\pm0.1)\times10^{-12}$	0.42 ± 0.11	$(2.2\pm0.1)\times10^{-12}$	0.69 ± 0.19

Stellar models suggest [3] that an accurate knowledge of the inverse reaction channel, ${}^{63}Ni(n,\gamma)$, is crucial for the production of ${}^{63,65}Cu$ and that a reduction of present cross section predictions by a factor of 2 is required to reproduce the Cu isotopes in their solar ratio. On the other hand, this reduction would also reduce the weak *s* process efficiency for heavier species along the neutron capture path up to $A\approx70$.

Our data are still preliminary and can give only hints but no definite answer. Thus we have to postpone a further discussion until results from the recently performed direct measurement of ${}^{63}Ni(n,\gamma)$ cross section using the time-of-flight method at the DANCE facility in Los Alamos are available [16].

References

[1] E. Burbidge, G. Burbidge, W. Fowler, and F. Hoyle, Rev. Mod. Phys. **29**, 547 (1957).

[2] Stephan Walter, Ph. D. thesis (Universität Karlsruhe) 2008; Wissenschaftliche Berichte FZKA-7411.

[3] M. Pignatari, *et al.,* Astrophys. J **710**, 1557 (2010).

[4] H. Nassar, *et al.,* Phys. Rev. Lett. **94**, 092504 (2005).

[5] Z.Y. Bao, *et al.,* At. Data Nucl. Data Tables **76**,70 (2000).

[6] The *"Karlsruhe Astrophysical Database of Nucleosynthesis in Stars"*, Version 0.3 (August 28th, 2009), Online: www.kadonis.org

[7] I. Dillmann, *et al.,* Nucl. Instr. and Meth. B **268**, 1283 (2009).

[8] A.M. Alpizar-Vicente, *et al.,* Phys. Rev. C**77**, 015806 (2008).

[9] T. Rauscher and F.-K. Thielemann, At. Data Nucl. Data Tables **75**, 1 (2000).

[10] F. Gabriel, *et al.,* , Nucl. Instr. Meth. B **161** , 1143 (2000).

[11] R. Schwengner, *et al.,* Nucl. Instr. Meth. A **555** 211 (2005).

[12] G. Rugel, *et al.,* Nucl. Instr. Meth. B **172**, 934 (2000).

[13] G. Rugel, *et al.,* Nucl. Instr. Meth. B **223**, 776 (2004).

[14] T. Rauscher and F.-K. Thielemann, At. Data Nucl. Data Tables **88**, 1 (2004).

[15] A. J. Koning, S. Hilaire, and M. Duijvestijn, Proc. *"Int. Conf. on Nucl. Data for Science and Technology- ND2007"*, Nice/France (April 2007), edts. O. Bersillon, F. Gunsing, R. Jacqmin, and S. Leray, EDP Science, 2008, p. 211-214; Online at www.talys.eu

[16] A. Couture, priv. comm. (2010).